Signature: © Pol J Radiol, 2014; 79: 75-78
DOI: 10.12659/PJR.889951

Polish Journal of Radiology
www.PolRadiol.com
ORIGINAL ARTICLE

Received: 2013.10.26
Accepted: 2013.12.12
Published: 2014.04.14

Authors' Contribution:
A Study Design
B Data Collection
C Statistical Analysis
D Data Interpretation
E Manuscript Preparation
F Literature Search
G Funds Collection

Distribution of the radiation dose in multislice computer tomography of the chest – phantom study

Tomasz Gorycki[1,2ABCDEF], Kamil Kamiński[2BCD], Michał Studniarek[1,2CDE], Przemysław Szlęzak[2DEF], Agnieszka Szumska[3B]

[1] Department of Radiology, Medical University of Gdańsk, Gdańsk, Poland
[2] Department of Imaging Diagnostics and Interventional Radiology, Franciszek Łukaszczyk Oncology Center in Bydgoszcz, Bydgoszcz, Poland
[3] Individual and Environmental Dosimetry Laboratory, Henryk Niewodniczański Institute of Nuclear Physics, Polish Academy of Sciences, Cracow, Poland

Author's address: Tomasz Gorycki, Department of Radiology, Medical University of Gdańsk, Dębinki 7 Str., 80-952 Gdańsk, Poland, e-mail: tgor@gumed.edu.pl

Summary

Background: The most commonly used form of reporting doses in multislice computed tomography involves a CT dose index per slice and dose-length product for the whole series. The purpose of this study was to analyze the actual dose distribution in routine chest CT examination protocols using an antropomorphic phantom.

Material/Methods: We included in the analysis readings from a phantom filled with thermoluminescent detectors (Art Phantom Canberra) during routine chest CT examinations (64 MDCT TK LIGHT SPEED GE Medical System) performed using three protocols: low-dose, helical and angio-CT.

Results: Mean dose values (mSv) reported from anterior parts of the phantom sections in low-dose/helical/angio-CT protocols were as follows: 3.74; 16.95; 30.17; from central parts: 3.18; 14.15; 26.71; from posterior parts: 3.01; 12.47; 24.98 respectively. Correlation coefficients for mean doses registered in anterior parts of the phantom between low-dose/helical, low-dose/angio-CT and helical/angio-CT protocols were 0.49; 0.63; 0.36; from central parts: 0.73; 0.66; 0.83, while in posterior parts values were as follows: 0.06; 0.21; 0.57.

Conclusions: The greatest doses were recorded in anterior parts of all phantom sections in all protocols in reference to largest doses absorbed in the anterior part of the chest during CT examination. The doses were decreasing from anterior to posterior parts of all sections. In the long axis of the phantom, in all protocols, lower doses were measured in the upper part of the phantom and at the very lowest part.

Keywords: Radiation Safety • Radiation Protection • Computed Tomography (CT) • Chest CT • Lung CT • Low Dose CT

PDF file: http://www.polradiol.com/download/index/idArt/889951

Background

The most common form of reporting the dose in multislice computed tomography is by declaring a mean dose for a single slice as a CT dose index volume or a dose for a given series as a dose-length product [1–3].

Standard method of determining the CT dose index volume on the basis of measurements on cylindrical phantoms results in underestimation of calculated dose for examined children and slim patients and dose overestimation in case of obese patients. The differences may reach 20% [2,3]. These methods do not convey information regarding actual dose distribution in particular parts of examined body part, which translates into a dose burden on particular organs [1–3].

The goal of this work was to analyze the radiation dose distribution within thoracic cavity during routine computed tomography examinations using an anthropomorphic phantom.

Material and Methods

We analyzed the dose values acquired from 3 sets of thermoluminescent detectors filling each phantom (Art Phantom Canberra) during routine chest CT examinations (64 MDCT TK LIGHT SPEED Medical Systems) performed in three successive protocols: low-dose, helical and angio-CT. Exposition parameters were the following: 1) low-dose CT lung examination (LDCT: 100kV, 30 mAs, slice thickness 1.5 mm), 2) helical examination (100 kV, slice thickness 5 mm), 3) angio-CT (120kV, slice thickness 1.25mm). Protocols 2 and 3 were performed with automatic selection of mAs.

In our study we used sections corresponding to the thorax of an anthropomorphic ART Phantom by Canberra Co. (Figure 1) that allows for installation of each group of neighboring sections from any part of the phantom. Fourteen phantom sections corresponding to an area of the chest were assembled, filled with detectors to be used in vertical position and joined together with connecting bars, which ensured the integrity of the phantom after filling it with detectors. Afterward, the assembled phantom was put in a horizontal position typical for computed tomography studies.

In each section phantom matrix contained orifices capable of accommodating detectors. Orifices were initially filled with inserts made of materials equivalent to tissues. Extractors and a number of special inserts enabling accommodation of TLD dosimeters were used to fit in the detectors. Commercially available thermoluminescent detectors in a form of LiF: Mf,Ti type pellets (MTS-N) were used. Each detector was given a number, which determined its fixed localization in a given section of a phantom during each scanning. An automatic RADOS 2000 reader was used to extract the readings (calibration and data extraction was performed by a certified IFJ laboratory in Cracow) [4].

We performed descriptive statistics, characterizing the quantitative variables using arithmetic means, standard deviations, medians, as well as minimal and maximal values. Subsequently, we assessed the statistical significance of obtained differences in mean dose values and evaluated the statistical significance of acquired correlation coefficients.

A Shapiro-Wilk test was used to check for normal distribution. Significance of differences between groups was verified using the F-test (ANOVA) or Kruskal-Wallis test (if conditions for ANOVA analysis were not met). If there were statistically significant differences between groups, post-hoc tests (Tukey, Dunn) were conducted. In all calculations $p=0.05$ was considered a cutoff point for statistical significance. All statistical calculations were performed using STATISTICA v. 10.0 (data analysis software system) StatSof, Inc. (2011) (www.statsoft.com) and Excel spreadsheet.

The following problems were taken into consideration: 1 – are there differences between the doses registered by the detectors in individual chest CT protocols, 2 – are there differences between mean dose values registered in the long axis of the phantom, 3 – are there differences between mean dose values registered in the short axis of the phantom in three areas of interest: anterior 1/3, middle 1/3 and posterior 1/3 of the cross-section of the thorax, 4 – is there a correlation between the distribution of doses registered according to the above described scheme in subsequent sections of the phantom in three various scanning protocols.

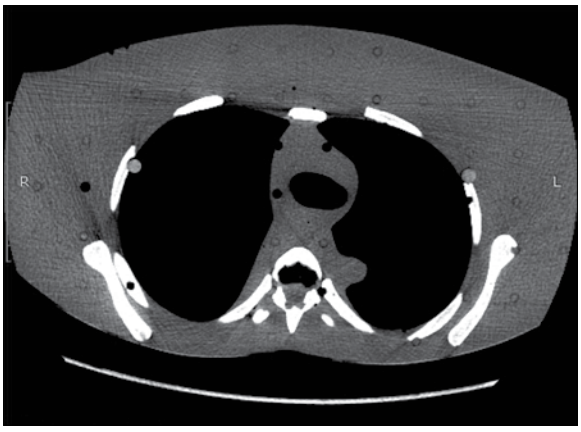


Figure 1. A computed tomography scan of a phantom.

Results

Statistical characteristics of the doses registered in particular phantom sections during three CT scanning protocols are displayed in Table 1. Dose distribution in the short axis of the phantom is presented in Figure 2.

Distribution of doses in the long axis of the phantom presented as mean doses in 14 subsequent phantom sections is displayed in Figure 3. Correlation coefficients describing the repeatability of distribution of mean dose values measured in anterior, middle and posterior sections of the phantom in various protocols are presented in Table 2. Statistical significance of differences between mean dose values and statistical significance of acquired correlation coefficients are noted in Tables 1 and 2.

Discussion

Established since 2002, widely accepted method of reporting the doses in computed tomography based on CT dose index volume for a given slice and a dose-length product for a total dose for entire series, is used for comparing initial doses previously measured on reference phantoms. They take into consideration exposition parameters, pitch factor, detector rotation time and filtration. They do not take into account patient size and body mass. They also do not convey any information on the distribution of doses in patient's body [5,6]. Use of anthropomorphic phantoms with particular sections mimicking the structure and proportions of a human body with regard to the density of specific organs and tissue regions allows for conducting simulations of clinical studies under conditions as close to reality as possible without exposing anyone to radiation risk. Due to the possibility of freely placing various types of detectors in successive cross-sectional slices of a phantom, it is possible to determine actual distribution of radiation burden in its particular parts.

A basic method of reducing the radiation dose for each patient during clinical CT examination involves narrowing

Table 1. Descriptive statistics concerning doses measured by detectors during scanning of the phantom and statistical significance of differences between mean dose values.

Protocol	Low-dose			Helical			Angio-CT		
	Section part			Section part			Section part		
Part of phantom's section	Anterior	Middle	Posterior	Anterior	Middle	Posterior	Anterior	Middle	Posterior
Dose (mSv)									
Mean	3.74	3.18	3.01	16.95	14.15	12.47	30.17	26.71	24.98
Min./max.	3.32 4.50	2.60 3.61	2.63 3.29	14.64 22.14	12.04 16.09	10.38 14.18	26.47 34.35	21.67 30.17	21.47 27.43
Median	3.66	3.24	3.04	15.99	14.53	12.57	30.26	27.04	25.33
Standard deviation	0.34	0.31	0.19	2.34	1.34	1.14	2.18	2.53	1.73
Statistical significance of differences between means (p)	0.0001		0.0429	0.0003		0.0007	0.0003		0.0222

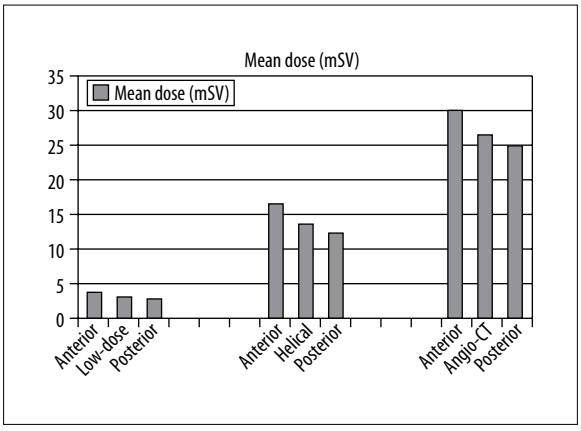


Figure 2. Dose distribution in the short axis of the phantom with a division into anterior, medial and posterior parts of phantom sections.

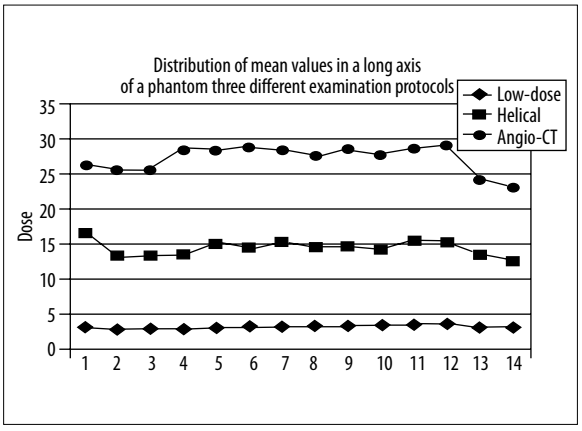


Figure 3. Dose distribution in the long axis of the phantom.

Table 2. Correlations between mean doses acquired from anterior, medial and posterior parts of the phantom in the course of three scanning protocols. Significant correlations with $p<0.05$ are denoted with*.

Correlation coefficient	Low-dose/helical	Low-dose/angio-CT	Helical/angio-CT
Anterior	0.49	0.63*	0.36
Middle	0.73*	0.66*	0.83*
Posterior	0.06	0.21	0.57*

of the scan range. However, in our material, scan range was identical during phantom scanning in all three protocols and thus, did not influence the results.

In everyday practice additional reduction in radiation exposure may be achieved by lowering of kV or mAs during scanning of slim patients, use of complex algorithms of radiation beam modulation, increasing the pitch factor and using various grades of noise filtration [7–11]. During the study, standard protocol parameters were not subject to modification.

In the present study we determined significant differences in mean doses measured by detectors during phantom scanning in various chest CT protocols. Mean doses registered during a low-dose scanning protocol constituted about 12% of those seen in an angio-CT protocol, while mean values registered during helical scanning protocol constituted 53% of those noted in angio-CT protocol. It was a natural consequence of the differences in exposition parameters attributed to particular chest CT protocols and different slice thickness.

Use of conversion coefficients dependent on the initial method of determining the CT dose index volume (e.g. phantom size) as well as size, weight and age of an actual patient help to estimate the dose at the central point of the layer passing through patient's body. Such estimate displays a tendency toward dose overestimation in relation to a real mean dose for a given layer [5,12]. It is mainly caused by an unequal initial dose generated during scanning of a given patient body volume, usually with a tendency for dose intensification in the central part of scanned volume with its increase [12,13]. This effect was observed during exposure analysis in the course of studies conducted on various types of multislice tomographs [6,9,12].

With regard to dose distribution in phantom's short axis in all phantom sections, in all scanning protocols the highest mean dose values were registered by detectors located in anterior parts of the phantom regardless of the size of a scanned cross-section. Decrease in mean dose registered sequentially in the middle and posterior parts of the phantom showed identical regularity. The greatest dose burden absorbed at the base of the breast near the anterior surface of the thorax during chest CT studies has been previously reported [11,12]. It might be affected by the geometry of table/patient body arrangement within the radiation beam, resulting in attenuation of radiation entering patient body from the dorsal side, as well as use of less than full angle during scanning [7,11,12]. Practical significance of those regularities for patient radiological safety with regard to radiological exposure of bone marrow and mammary gland is such that one should consider placing the patient in a prone position during the study, particularly in case of patients undergoing frequent, repeated CT examinations and those, in whom radiological burden on the red bone marrow is particularly important, e.g. in patients with hematological disorders. Analyzing the distribution of dose burden in phantom's long axis, in all study protocols we observed relatively lower mean doses in the upper phantom sections corresponding to the plane of thoracic inlet and upper lung fields, as well as an increase in measured doses in the central parts of the phantom with a drop in the lower sections of a phantom. Such dose distribution is most likely due to the predominance of lower-density tissue in the upper part of the chest caused by the predominance of lung tissue volume over relatively small cross-section of superior mediastinum and the response of the scanner to tissue density measurements from the scanograms, translating into the influence of dose modulation on lower doses in the upper part of patient's chest [2,5,9,12]. In the middle and lower part of thoracic cavity we observe an increase in the absolute volume of all tissues and an increase in relatively higher density of mediastinum in cross-sectional imaging. Some impact on registering lower mean values by detectors located on the lower margin of the phantom relative to those reported in studies on whole-body phantoms may be due to the lack of influence of dispersed radiation coming from epigastrum [5,6,12].

Assessing the correlation between mean doses in particular parts of the phantom in various scanning protocols, only in the middle part of phantom's section did we observe similar distribution of mean values among consecutive scanning protocols (Table 2). It might be influenced by previously mentioned effect of dose accumulation in the central part of the phantom together with increasing volume of scanned area, which is helpful in detecting similarities in dose distribution during scanning, as well as the number of detectors in the middle part of phantom section ensuing from its structure [5,6,12].

Conclusions

In multislice computed tomography of the chest, dose burden in the short axis of the body predominates in the part of the chest that is directed upward, which practically translates into greatest dose burden absorbed in the anterior part of the thorax in a patient lying in supine position and predominating dose burden in the dorsal part of the thorax in a patient lying in a prone position during examination.

We observed a tendency toward reduction of measured doses from the anterior part of the phantom, through the middle parts of the section, to the lowest doses in the posterior part of the phantom.

In all study protocols we observed lower mean doses in the upper phantom sections corresponding to upper lung fields and an increase in measured doses in central parts of the phantom with a drop in lower sections of a phantom.

References:

1. Cody DD, Kim HJ, Cagnon CH et al: Normalized CT dose index of the CT scanners used in the National Lung Screening Trial. Am J Roentgenol, 2010; 194: 1539–46
2. Kalra MK, Maher MM, Toth TL et al: Strategies for CT radiation dose optimization. Radiology, 2004; 230: 619–28
3. Huda W, Ogden KM, Khorasani MR: Converting dose-length product into effective dose. Radiology, 2008; 248: 995–1003
4. Niewiadomski T: 1996. 25 Years of TL Dosimetry at the Institute of Nuclear Physics, Kraków, Radiation Protection Dosimetry, 1996; 65: 1–6
5. McCollough CH, Bruesewitz MR, Kofler JM Jr: CT dose reduction and dose management tools: Overview of available options. Radiographics, 2006; 26: 503–12
6. McCollough CH, Leng S, Yu L: CT dose index and patient dose: they are not the same thing. Radiology, 2011; 239: 311–16
7. Singh S, Kalra MK, Hsieh J et al: Abdominal CT: Comparison of adaptive statistical iterative and filtered back projection reconstruction techniques. Radiology, 2010; 257: 373–83
8. Hara AK, Paden RG, Silva AC et al: Iterative reconstruction technique for reducing body radiation dose at CT: Feasibility study. Am J Roentgenol, 2009; 193: 764–71
9. Leipsic J, Nguyen G, Brown J et al: A prospective evaluation of dose reduction and image quality in chest CT using adaptive statistical iterative reconstruction. Am J Roentgenol, 2010; 195: 1095–99
10. Prakash P, Kalra MK, Digumarthy SR et al: Radiation dose reduction with chest computed tomography using adaptive statistical iterative reconstruction technique: Initial experience. J Comput Assist Tomogr, 2010; 34: 40–45
11. Tack D: Radiation Safety in Thoracic Imaging. European Cardiology, 2009; 7: 19–22
12. Fujii K, Aoyama T, Yamamauchi-Kawaura C: Radiation dose evaluation in 64-slice CT examinations with adult and paediatric anthropomorphic phantoms. Brit J Radiol, 2009; 82, 1010–18